***Final Draft***
**of the original manuscript:**

Behl, M.; Lendlein, A.:
**Shape Memory Polymers**
In: Materials Today (2007) Elsevier

DOI: 10.1016/S1369-7021(07)70047-0

# Shape-Memory Polymers: Dual Shape Materials for Biomedical Applications

Marc Behl, Andreas Lendlein*
Center for Biomaterial Development, Institute of Polymer Research, GKSS Research Center Geesthacht, Kantstr. 55, D-14513 Teltow, Germany.
* To whom correspondence should be addressed. E-mail: andreas.lendlein@gkss.de

## *Abstract*

Shape-memory polymers are an emerging class of active polymers, having dual shape capability. They can change their shape in a predefined way from shape (A) to a shape (B) when exposed to an appropriate stimulus. While shape (B) is given by the initial processing step, shape (A) is determined by applying a process called programming. In this paper fundamental aspects of the molecular design of suitable polymer architectures, tailored programming and recovery processes and the quantification of the shape-memory effect are presented. Shape-memory research was initially founded on the thermally-induced dual shape-effect. This concept was extended to other stimuli by either indirect thermal actuation or direct actuation by addressing stimuli-sensitive groups on the molecular level. Finally, polymers are introduced which can be multifunctional. Besides their dual shape capability theses active materials are biofunctional or biodegradable. Potential applications for such materials as active medical devices are highlighted.

## 1. Introduction

Shape-memory polymers are an emerging class of polymers with applications spanning over various areas of every-day life. Such applications can be found e.g. in smart fabrics [1, 2], heat-shrinkable tubes for electronics or films for packaging [3], self-deployable sun sails in space crafts [4], self-disassembling mobile phones [5], intelligent medical devices [6] or implants for minimally invasive surgery [7, 8]. As these enumerations cover only a small amount of possible applications and from the authors point of view the shape-memory technology bears the potential of numerous other applications, fundamental aspects of the shape-memory effect are presented.
Shape-memory polymers are dual shape materials belonging to the group of actively moving polymers [9]. They can actively change from a shape (A) to a shape (B). Shape (A) is a temporary shape, which is obtained by mechanical deformation and subsequent fixation of that deformation. This process also determines the change of shape shift, resulting in the shape (B), which is the permanent shape. In shape-memory polymers reported so far, heat or light has been used as stimulus. By the use of irradiation with IR-light, application of electric fields, alternating magnetic fields or immersion in water, indirect actuation of the shape-memory effect has been realized. The shape-memory effect relies only on the molecular architecture and does not require a specific chemical structure of the repeating units. Therefore intrinsic material properties e.g. mechanical properties can be adjusted to the need of specific applications by variation of molecular parameters such as the type of monomer or the comonomer ratio.

## 2. General Concept of Shape-Memory Polymers

The shape-memory effect is not an intrinsic property, meaning polymers do not display this effect by themself. Hence, enabling of the shape-memory effect is an aimed combination of polymer morphology and a specific processing and has to be understood as a polymer functionalization. By conventional processing e.g. extruding or injection molding, the polymer is formed into its initial permanent shape (B). Afterwards, in a process called programming the polymer sample is deformed and fixed in the temporary shape (A). Upon application of an external stimulus the polymer recovers into its initial permanent shape (B). This cycle of programming and recovery can be repeated several times, with different temporary shapes in subsequent cycles. In comparison to metallic shape-memory alloys this cycle of programming and recovery can take place in a much shorter time interval and polymers allow a much higher deformation rate between shapes (A) and (B) [10].

Shape-memory polymers are elastic polymer networks, which are equipped with suitable stimuli-sensitive switches [11, 12]. The polymer network consists of molecular switches and netpoints (figure 1). The netpoints determine the permanent shape of the polymer network and can be of chemical (covalent bonds) or physical (intermolecular interactions) nature. Physical crosslinking is obtained in a polymer, whose morphology consists of at least two segregated domains, as found for example in block copolymers. Here, the domains related to the highest thermal transition temperature ($T_{perm}$) are acting as netpoint (hard segment), while the chain segments associated to the domain with the second highest thermal transition $T_{trans}$ are acting as molecular switches (switching segment). If the working temperature is higher than $T_{trans}$ then switching domains are flexible resulting in an entropy elastic behavior of the polymer network above $T_{trans}$. If the sample has been previously deformed by applica-

tion of an external stress, it snaps back into its initial shape, once the external stress is released. The molecular mechanism of the shape-memory effect is illustrated in figure 1 for the thermally-induced shape-memory effect. The shape-memory polymer network consists of covalent netpoints and switching segments based on physical interaction.

Figure 1

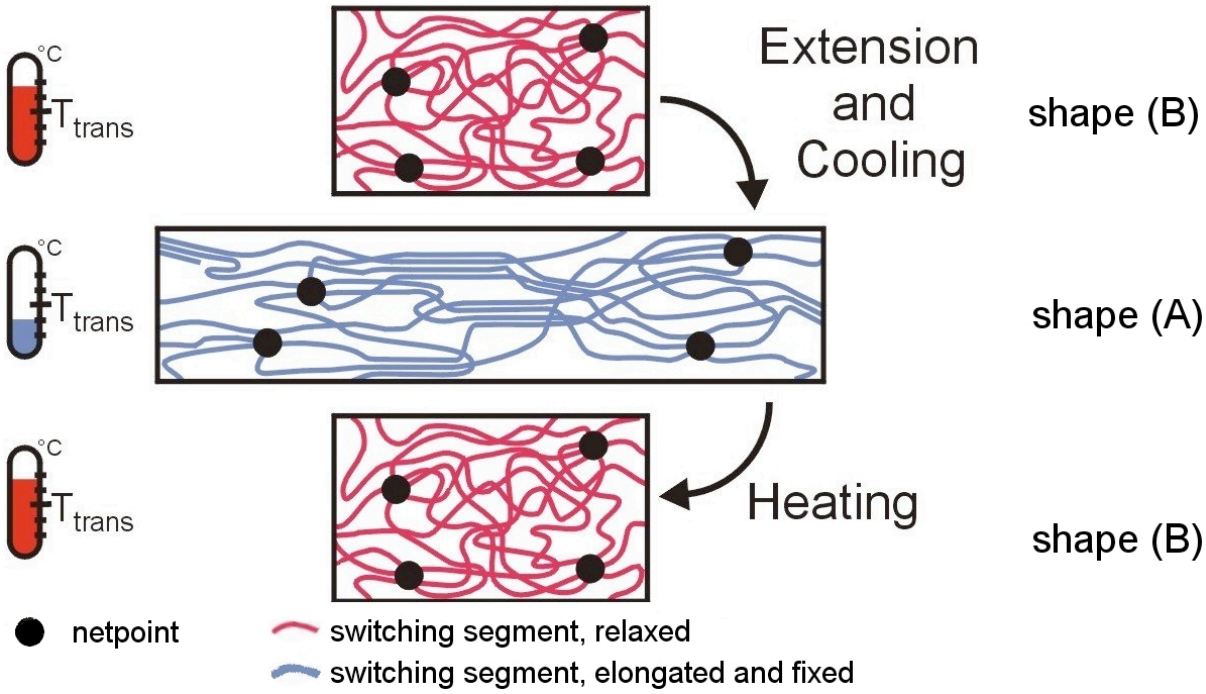


Figure 1 Molecular mechanism of the thermally-induced shape-memory effect
$T_{trans}$= thermal transition temperature related to the switching phase (adapted from [11])



To display shape-memory functionality, the polymer network has to be temporarily fixed in a deformed state under environmental conditions relevant for the particular application. This requires the reversible prevention of the recoiling of the under external stress deformed chain segments and is achieved by the introduction of reversible netpoints as the molecular switches. These additional netpoints can be formed by physical interactions or by covalent bonds. Physical crosslinking is obtained by vitrification or crystallization of domains related to $T_{trans}$. These switching domains can be formed either by either the chain segments driving the entropic elastic behavior themselves or by side chains, whose aggregation is able to temporarily prevent recoiling of that chains side chains or the side chain segments themselves. Reversibly covalent crosslinking is obtained by the attachment of functional groups to the chain segments. Controlled by an external stimulus, these functional groups must

be able to form reversibly covalent bonds by the reaction with each other or suitable counterpart functional groups.
Most of the shape-memory polymers reported so far use heat as stimulus. Here the stimulation results from the thermally-induced cleavage of the additional crosslinks mentioned above. If these additional crosslinks are based on physical interaction, a further distinction according to $T_{trans}$ can be made, which can be either glass transition $T_g$ or a melting temperature $T_m$. While $T_g$s are extending over a broad temperature interval, the latter ones can show a transition in a relatively small temperature interval. If these crosslinks are functional groups able to undergo photoreversible reactions, the shape-memory technology is extended to light as stimulus. Other stimuli like electrical current or electro-magnetic fields are used for the indirect heating of the material.

Figure 2

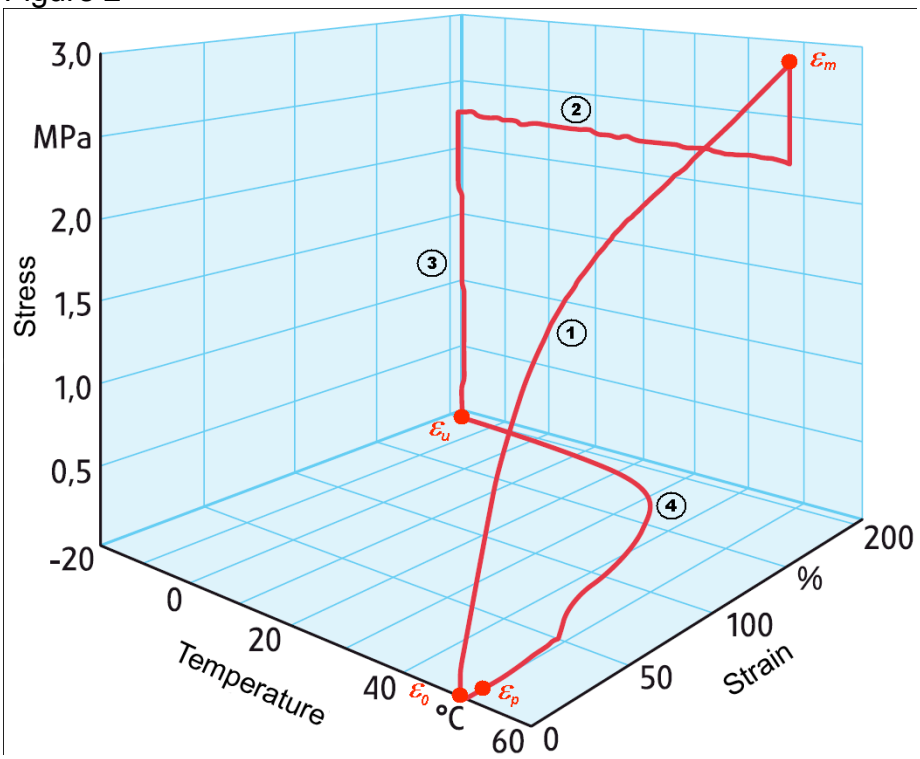


Typical stress-strain temperature diagram (first cycle) for a thermo-plastic shape-memory polymer with a thermally-induced shape-memory effect [7, 81]. Step 1 of the experiment is strain controlled, while steps 2 through 4 to the beginning of the next cycle are stress-controlled (adapted from [81]).



Shape-memory properties are quantified in cyclic mechanical tests being specific for the different stimuli [11-13]. As most stimuli are based on heat or light, thermo- or photomechanical test procedures have been developed. In these cyclic tests the strain fixity rate $R_f$, the strain recovery rate $R_r$ and in case of thermal stimulation the switching temperature $T_{switch}$ are determined, allowing the quantification of the shape-memory effect. For each number of cycles (N), $R_f$ quantifies the ability to fix a mechanical deformation $\varepsilon_m$, resulting in a temporary shape $\varepsilon_u(N)$. $R_r$ quantifies the abil-

ity to store a mechanical deformation after application of a certain deformation $\varepsilon_m$, as it builds the ratio between the change in strain recorded during shape-memory effect $\varepsilon_m$-$\varepsilon_p(N)$ and the change in strain in the course of programming given by $\varepsilon_m$-$\varepsilon_p(N-1)$. From the given equations it is obvious, that ideally $R_f$ and $R_r$ would be 100%.

$$R_f(N) = \frac{\varepsilon_u(N)}{\varepsilon_m} \qquad (1)$$

$$R_r(N) = \frac{\varepsilon_m - \varepsilon_p(N)}{\varepsilon_m - \varepsilon_p(N-1)} \qquad (2)$$

In a typical stress controlled programming cycle (figure 2) the test specimen is clamped into the tensile tester, the sample is elongated to $\varepsilon_m$ while the molecular switches are open (step 1). Opening of the molecular switches is realized in thermally-induced shape-memory materials by heating to a temperature $T_{high}$ above $T_{trans}$ and in light-induced shape-memory materials by irradiation having suitable wavelengths $\lambda_1$ to cleave photosensitive bonds. This strain is maintained for some time, to allow relaxation of the polymer chains and afterwards the experiment is continued in stress-controlled mode. While being held under constant stress $\sigma_m$ this temporary shape is fixed by closing of the molecular switches (step 2). Closing of the switches occurs in thermally-induced shape-memory materials by controlled cooling to a temperature below $T_{trans}$ or in light-induced shape-memory materials by irradiation with other suitable wavelengths $\lambda_2$. Afterwards the strain is reduced until a stress-free condition is achieved at 0 MPa (step 3). Finally, the molecular switches are opened again, while the tensile stress is held constant at 0 MPa, resulting in the contraction of the test specimen and resuming of its permanent shape (step 4).

Several models for the prediction of the shape-memory effect have been described [14-17]. They all base on uni-axial deformation processes but differ in their modelling approach. These approaches are based either on a mechanic modeling approach [14, 17] or a thermodynamic approach [15, 16]. They allow the prediction of irrecoverable strain [14, 16], temperature dependent stress and strain [15] or stress and strain [17] for polymers under deformation.

## *3. Thermally-induced Shape-Memory Effect*

### 3.1 Examples for polymers having a thermally induced shape-memory efect

An important group of physically crosslinked shape-memory polymers are linear block copolymers. Block copolymers with $T_{trans} = T_m$ are reviewed in [11], include polyurethanes and polyetherester. In polyesterurethanes the urethane segments are acting as hard segments, while poly($\varepsilon$-caprolactone) ($T_m$ = 44 – 55 °C) is forming the switching segment [18-20]. Additionally, polyesterurethanes containing mesogenic moieties have been reported [21, 22]. In block copolymers with *trans*-(polyisoprene) switching segments and urethane hard segments the microphase separation has been investigated [23]. Here the polyurethane segments are acting as physical crosslinks and assemble into spherical domains. $T_{trans}$ is based on a melting transition of the trans-(polyisoprene) switching segments.
In block copolymers the shape-memory effect can also be based on a glass transition temperature ($T_{trans} = T_g$). A typical example are polyurethanes whose switching domains are in most cases mixed phases [24].

Another class of thermoplastic shape-memory polymers whith $T_{trans} = T_g$ are polyesters. In co-polyester based on poly(ε-caprolactone) and poly(butylene terephthalate), the poly(butylene terephthalate) segments are acting as physical crosslinkers [25]. The shape-memory capability can also be added to a polymer by polymer analogous reaction. A polymer analogous reaction is the application of a standard organic reaction (like the reduction of a ketone to an alcohol) to a polymer having several of such reactive groups. An example is the polymer analogous reduction of an polyketone with $NaBH_4$/THF resulting in a poly(ketone-*co*-alcohol) [26]. The polyketones were synthesized by late transition metal catalyzed polymerization of propene, hex-1-ene or a mixture of propene and hex-1-ene with carbon monoxide. The $T_g$ of this polymer is directly related to the degree of reduction, which can be adjusted by the amount of $NaBH_4$/THF. The most promising shape-memory material was a partly reduced poly(ethylene-*co*-propene-*co*-carbonoxide), which displayed a phase-separated morphology with hard mirco-crystalline ethylene/ CO-rich segments within a softer amorphous polyketone ethylene-propene/CO-rich matrix. The crystalline domains of this material work as physical crosslinkers. This results in an elastic behavior above $T_g$ as the glass transition temperature ($T_{trans} = T_g$) is related to the switching phase. Partial reduction of the material allows control of the $T_g$, which could be adjusted between below room temperature and 75 °C.

Covalently crosslinked polymers can be obtained by crosslinking during synthesis or post polymerization methods. The post polymerization methods involve radiation and chemical methods. As an example dual shape capability can be added to polyethylene [3] and its copolymers [27, 28] by crosslinking with ionizing radiation (γ-radiation, neutrons). Radiation-crosslinking of poly(ε-caprolactone) results mostly in molecular chain scission and loss of useful mechanical properties [29]. By blending poly(ε-caprolactone) with polymethylvinylsiloxane, radiation crosslinking of the blend can be achieved and shape-memory properties can be added to the material [30]. Another option is the chemical crosslinking of poly[ethylene-*co*-(vinylacetate)] with dicumylperoxide as radical initiator [31]. The same radical initiator has been used for the crosslinking of semi-crystalline polycyclooctene [32]. A covalently crosslinked polymer from a natural source is a material which has been prepared by cationic polymerization of soybean oil with styrene and divinylbenzene, norbornadiene or dicyclopentadiene as crosslinker [33]. A material consisting of 45 wt% soybean oil, 27 wt% styrene and 17 wt% divinylbenzene (and 5 wt% Norway pronova fishoil and 3 wt% boron trifluoride diethyl etherate) displayed in bending tests 97% strain fixity and 100% shape recovery.

Figure 3

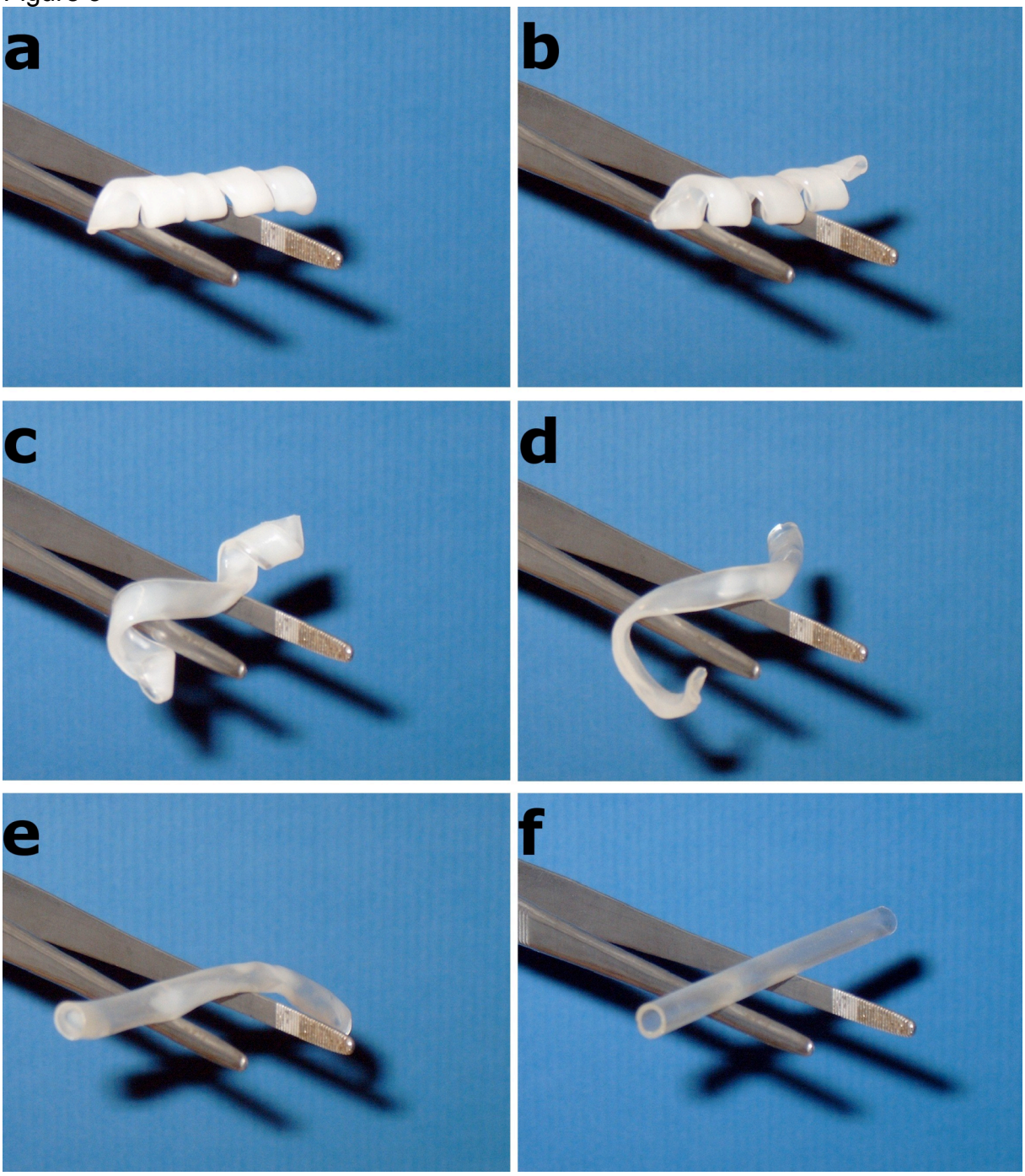


Time series of photographs showing recovery of a shape-memory tube. a–f, Start to finish of the process; total time, 10 s at 50 °C. The tube was made of a poly(ε-caprolactone)dimethacrylate polymer network (the $M_n$ of the network's switching segments was $10^4$) that had been programmed to form a flat helix. (taken from [59])



Synthesis of covalently crosslinked polymer networks during polymerization can be realized by (co)condensation or poly(co)condensation of one or several monomers, whereby at least one is trifunctional or by copolymerization of monofunctional mono-

mers with low-molecular weight or oligomeric crosslinkers. An example for the latter is a copolymer of stearyl acrylate, methacrylate and N,N- methylenebisacrylamide as crosslinker [34]. Here crystalline domains of stearyl side chains form the switching phase. In multiphase copolymer networks obtained by the radical polymerization of copolymerization of poly(octadecyl vinyl ether)diacrylates or –dimethacrylates with butyl acrylate as comonomer, the situation is similar [35, 36]. In both cases the crystalline domains of octadecyl side chains are acting as switching segments again.
An example of crosslinked polymer networks synthesized by (co)condensation respectively polyaddition of monofunctional monomers with low-molecular weight or oligomeric crosslinkers have been realized in polyurethanes by the addition of trimethylol to the reaction mixture [37].
Reaction of tetrafunctional silanes, working as netpoints, with oligomeric silanes, which work as spacers and to whom two distinct benzoate-based mesogenic groups have been attached, results in formation of main-chain smectic-C elastomer [38]. In contrast to other liquid crystalline elastomers, which display a shape-changing behavior and which have been compared to shape-memory polymers recently [9], these elastomers have shape-memory properties. The crosslink process during synthesis defines the permanent shape. The shape-memory effect is triggered by the thermal transition of the liquid crystalline domains. In the programming process the polymer network is heated to the isotropic state of the liquid crystalline domains, stretched or twisted and then cooled below the clearing transition temperature of the smectic-C mesogens. Upon reheating over this clearing transition the permanent shape can be recovered. In contrast to shape-changing liquid crystalline elastomer systems, these polymers display shape-memory behavior, as the liquid crystalline moieties are working as switch. In shape-changing liquid crystalline elastomers, the molecular movement of the single liquid crystals is converted into a macroscopic movement.

## 3.2 Indirect actuation of the thermally-induced shape-memory effect

Indirect actuation of the shape-memory effect has been realized by two different strategies. One method involves the indirect heating, e.g. by irradiation. The other possibility is lowering of $T_{trans}$ by diffusion of low molecular weight molecules into the polymer, working as plasticizer. This allows the triggering of the shape-memory effect, while the sample temperature remains constant.

Figure 4

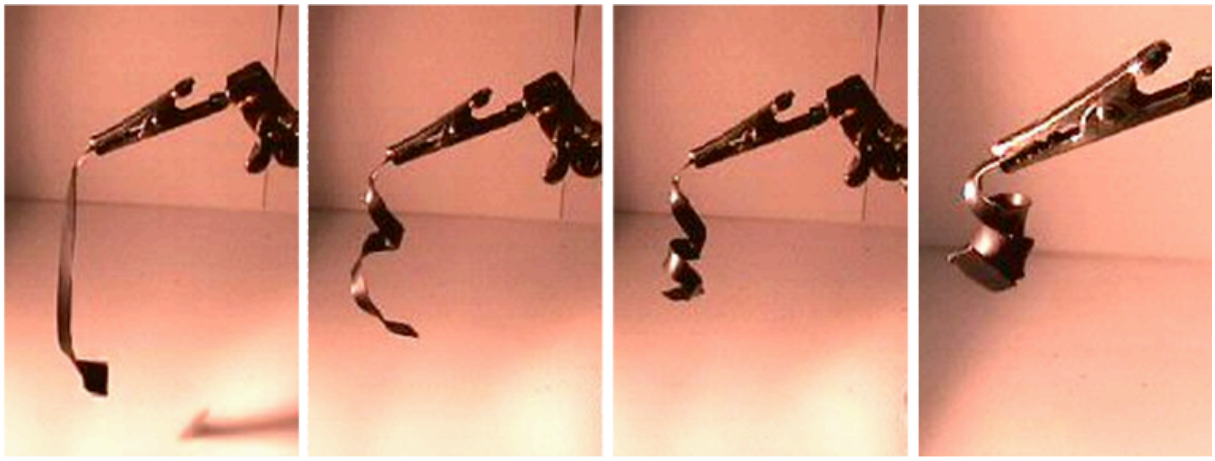

Strain recovery towards an infrared source. Infrared absorption, non-radiative energy decay and resulting local heating is constrained to the near-surface region of a stretched ribbon, resulting in strain recovery of the near-surface region and curling of the ribbon towards the infrared source (exposure from the left) within 5 seconds. (taken from [48])



Instead of increasing the environmental temperature, thermally-induced shape-memory polymers can be heated by illumination with infrared light. This concept was demonstrated in a laser-activated medical device from polyurethane [39, 40]. In such devices heat transfer can be enhanced by incorporation of conductive fillers such as conductive ceramics, carbon black and carbon nanotubes (figure 4) [41-43]. This incorporation of particles additionally influences mechanical properties: incorporation of microscale particles results in increased stiffness and recoverable strain levels [44, 45] and can be further enhanced by the incorporation of nano-scale particles [46, 47]. To reach an enhanced photothermal effect, the molecular structure of the particles has to be considered. Polyesterurethanes reinforced with carbon nanotubes or carbon black of similar size displayed increased strain and fixity [48]. While carbon black reinforced materials showed limited shape recovery around 25 – 30%, in carbon-nanotube reinforced polymers $R_f$s of almost 100% could be determined and had been attributed to a synergism between the anisotropic carbon nanotubes and the crystallizing polyurethane switching segments.

A certain level of conductivity can be reached by the incorporation of carbon nanotubes into shape-memory polyurethanes [49]. Upon application of an electrical current the sample temperature is increased, being caused by the high ohmic resistance of the composite. This effect has been used to trigger the shape-memory effect.

Incorporation of magnetic nanoparticles of iron(III)oxide cores in a silica matrix into shape-memory thermoplasts enables remote actuation of the thermally-induced shape-memory effect in magnetic fields (figure 5) [50]. Here the sample temperature is increased by inductive heating of the nanoparticles in an alternating magnetic field ($f$ = 258 kHz, $H$ = 7 - 30 $kA \cdot m^{-1}$). Two different thermoplastic materials have been used as matrix. The first material was an aliphatic polyetherurethane (TFX) from methylene bis(*p*-cyclohexyl isocyanate), butanediol and polytetrahydrofuran, while

the other was a biodegradable multiblock copolymer (PDC) with poly(*p*-dioxanone) as hard and poly(ε-caprolactone) as switching segment. While TFX has an amorphous switching phase, PDC has a crystallizable switching segment. Indirect magnetic actuation has been also realized by the incorporation of nickel zinc ferrite particles into a commercial ester-based thermoset polyurethane [51].

Figure 5

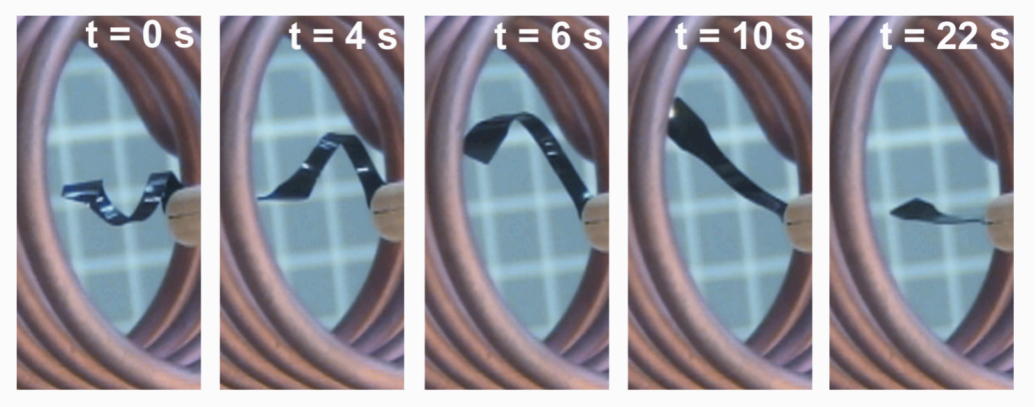


Magnetically-induced shape-memory effect of a thermoplastic shape-memory composite from nano-particles consisting of iron(III)oxide particles in a silica matrix and a polyetherurethane. (taken from [50])

R. Mohr, K. Kratz, T. Weigel, M. Lucka-Gabor, M. Moneke, and A. Lendlein. *PNAS*, 2006, **103**, 3540-3545. Copyright 2006 National Academy of Sciences, U.S.A

Indirect actuation of the shape-memory effect by lowering $T_{trans}$ has been shown for commercially available polyurethanes [52-54] and its composites with carbon nanotubes [55]. In all cases the temporary shape has been programmed by conventional methods for thermally-induced shape-memory polymers. When immersed into water, moisture diffuses into the polymer sample and acts as plasticizer, resulting in shape recovery (figure 6). In the polymers and composites based on polyurethanes the $T_g$ is lowered from 35 °C to a temperature below ambient temperature. It could be shown, that the lowering of the glass transition temperature depends on the moisture uptake which depends on the immersion time. In time dependent immersion studies, it was shown, that the water uptake could be adjusted between 0 and 4.5 wt% which goes along with a lowering of $T_g$ between 0 and 35 K. As the maximum moisture uptake achieved after 240h was around 4.5 wt% this shape-memory polymer still has to be understood as a polymer and not as a hydrogel. A different strategy of water actuated shape-memory polymers was realized in polyetherurethane polysilesquisiloxane block copolymers [56]. Here, low molecular weight poly(ethylene glycol) has been used as polyether segment. Upon immersion in water, the poly(ethylene glycol) segment gets dissolved, resulting in the disappearance of $T_m$ and recovery of the permanent shape.

Figure 6

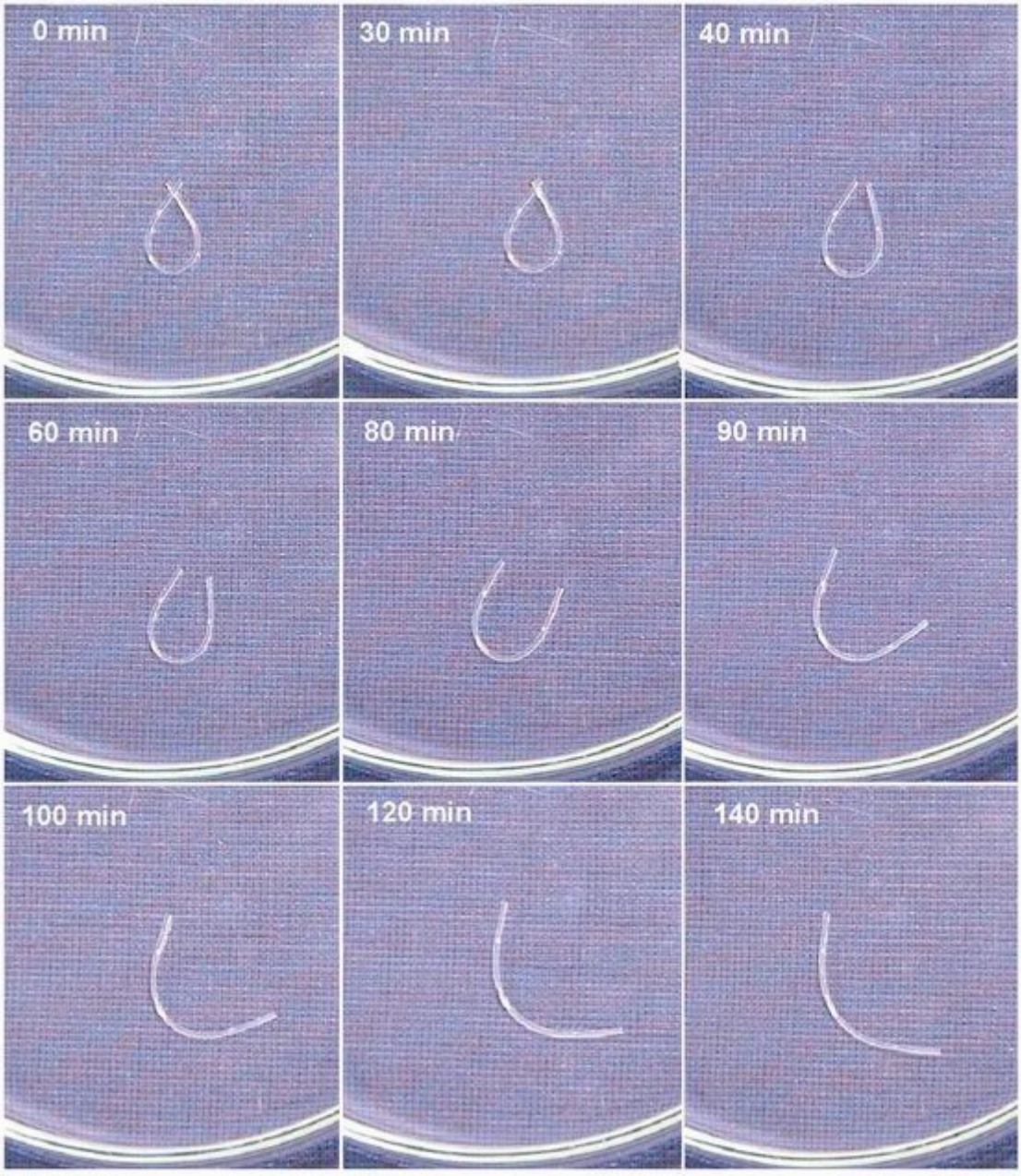


Water driven actuation of a shape-memory effect: The shape-memory polyurethane in circular temporary shape is immersed into water. After 30 min the recovering of the linear permanent shape starts.



## *4. Light-induced Shape-Memory Effect*

By the incorporation of reversibly photoreacting molecular switches, light-induced stimulation of shape-memory polymers have been realized [13, 57, 58]. This stimulation is independent of any temperature effects and must be differentiated from the indirect actuation of the thermally-induced shape-memory effect.

Figure 7

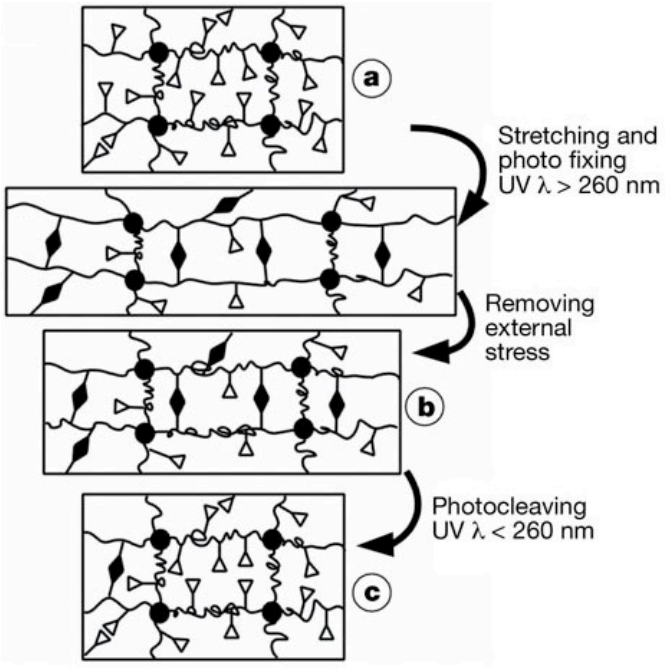


Molecular mechanism of light-induced shape-memory effect of a grafted polymer network: the chromophores (open triangles) are covalently grafted onto the permanent polymer network (filled circles, permanent crosslinks), forming photoreversible crosslinks (filled diamonds); fixation and recovery of the temporary shape are realized by UV light irradiation of suitable wavelengths. (taken from [57])



To introduce sensitivity to light into shape-memory polymers, cinnamic acid (CA) or cinnamylidene acetic acid (CAA) moieties were incorporated into the polymer architecture, which are working as light-triggered switches and which is illustrated in figure 7 [57]. Upon irradiation with light having suitable wavelengths, a [2 + 2] cycloaddition reaction occurs between two of these light-sensitive moieties, forming a cyclobutane-ring and in this way covalent crosslinks. Irradiation with different suitable wavelengths results in cleavage of the newly formed bonds.
Two alternative strategies were realized for the molecular structure of the light sensitive-polymers: a graft polymer and an interpenetrating polymer. For the graft polymer, CA molecules were grafted onto a permanent polymer network which has been realized by copolymerization of n-butylacrylate, hydroxyethyl methacrylate and ethylene-gylcol-1-acrylate-2-CA and poly(propylene glycol)-dimethacrylate) (Mn = 560 $g \cdot mol^{-1}$) as crosslinker. Loading a permanent polymer network from butylacrylate and 3 wt% poly(propylene glycol)-dimethylacrylate ($M_n$ = 1000 $g \cdot mol^{-1}$) as crosslinker with 20 wt% star-poly(ethylene glycol) end capped with terminal CAA groups yields the photosensitive interpenetrating network. In both cases the permanent shape is determined by the crosslinks of an amorphous polymer network. In the programming cycle, the polymer is stretched first, resulting in a strain of the coiled polymer segments. Afterwards, the network is irradiated with UV-light > 260 nm, creating new covalent

netpoints, which fix the strained form in a temporary shape. The permanent shape recovers upon irradiation with UV-light of $\lambda < 260$ nm, as the crosslinks are cleaved.

## *5. Biomedical Applications of Shape-Memory Polymers*

Figure 8

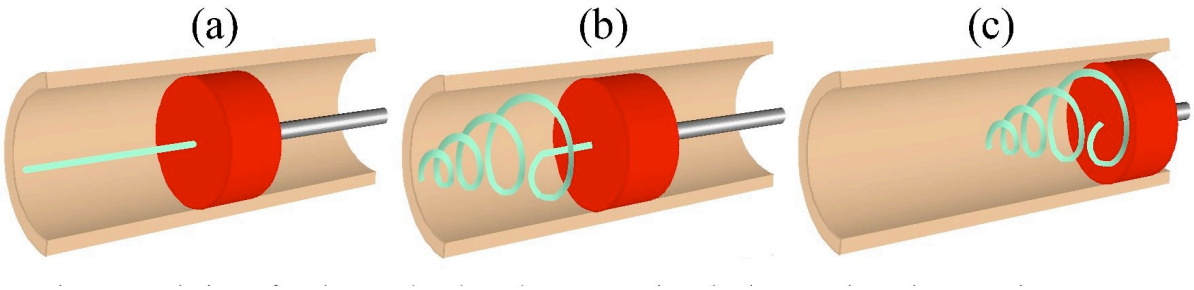


Depiction of endovascular thrombectomy using the laser-activated SMP microactuator coupled to an optical fiber. (a) In its temporary straight rod form, the microactuator is delivered through a catheter distal to the blood clot. (b) The microactuator is then transformed into its permanent corkscrew form by laser heating. (c) The deployed microactuator is retracted to capture the thrombus. (taken from [40])



An attractive application area for shape-memory polymers is their use in active medical devices within the field of medicine [59, 60]. Here, first examples have been realized in an laser activated device for the mechanical removal of blood clots (figure 8) [39, 40]. The device is inserted by minimally invasive surgery into the vessel and upon laser activation the shape-memory material coils into its permanent shape, enabling the mechanical removal of the thrombus. Another example for a medical challenge to be addressed is the curing of obesity which is one of the major health problems of developed countries. In most cases overeating is the key problem, which can be circumvented by methods for curbing appetite. A solution for this may be biodegradable intragastric implants, which inflate after an approximate predetermined time and provide the patient with a feeling of satiety after only small amount of food have been eaten [61, 62].

Shape-memory foams have been proposed as measuring device, which surveys the shape of an human ear canal, so that an hearing aid can be fitted properly [63]. The material is commercially available polyurethane foam having a $T_g$ as switching transition. The foam shows full recovery at 83% compression. Another application of shape-memory polymers is the use as stents for the prevention of strokes [64]. Here, coils of a composite consisting of tantal and a polyetherurethane ($T_{trans} = T_g$ ; $T_g = 33$ °C) have been studied. Tantal is needed as radio-opaque filler for diagnostic detection. It could be shown that the filling does not affect the shape recovery behavior but lowers $T_g$ and maximum recovery stress.

When polyurethane based shape-memory polymers are used in vivo, biocompatibility and cytotoxicity have to be considered. In an in vitro study it could be shown, that commercially available aromatic shape-memory polyetherurethanes have similar bio-

compatibility and cytotoxicity compared to non-shape-memory polyurethanes [65]. Furthermore it was demonstrated, that cell adhesion and cell growing could be promoted by protein coating and cell platelet adhesion and reactivity was low.

## 5.2 Biodegradable Shape-Memory Polymers

Besides different ways of stimulation, biodegradability would be benefitial for many medical applications [60]. The intended combination of shape-memory capability and biodegradability is an example for multifunctionality of a material [66]. This type of multifunctionality especially adds advantage to medical devices for minimally invasive surgery. These polymers allow the insertion of bulky implants in a compressed shape into the human body through a small incision. When stimulated within the body they turn into their application relevant shape. Another example is a biodegradable shape-memory polymer as intelligent suture for wound closure [7]. Upon actuation of the shape-memory effect, the material is able to apply a defined stress to the wound lips (figure 9). In both applications the removing of the implant in a follow-on surgery is not necessary, as it degrades within a predefined time interval.
Biodegradability of shape-memory polymers can be realized by the introduction of weak hydrolizable bonds, which cleave under physiological conditions. Generally biodegradable polymers can be classified into surface and bulk eroding polymers [67]. While the first ones present a linear degradation characteristic, the latter ones show a non-linear degradation. When diffusion of water into the polymer sample besides the reactivity of the polymer functional groups is taken into account, the degradation type can be predicted [68]. Table 1 gives an overview about degradable shape-memory polymers for potential biomedical applications.

Table 1 Biodegradable Shape-Memory Polymers

| polymer | | shape-memory properties | degradation properties 50% / complete | biocompatibility *in vitro* | biocompatibility *in vivo* |
|---|---|---|---|---|---|
| poly(ε-caprolactone) dimethacrylate and n-butyl acrylate | 71, 72 | third cycle<br>$R_f$ 93 - 98%<br>$R_r$ ~ 95% | phosphate buffer solution (pH 7.4; 37 °C)<br>no mass loss after 140 d | statistically significant differences in the cell lysis depending on sterilization technique | CAM-test<br>no adverse effects on the angiogenesis |
| star-shaped oligoesters of *rac*-dilactide and diglycolide | 75 | fifth cycle<br>$R_r \leq 97\%$<br>$R_f \geq 99\%$ | aqueous buffer solution (pH 7; 37°C)<br>80 d / 150 d | no data shown | no data shown |
| multiblock copolyesters from poly(ε-caprolactone) and poly(ethlene glycol) and chain extender based on cinnamic acid groups | 76 | [i]<br>third cycle<br>$R_f$ = 100%<br>$R_r$ = 88% | [ii]<br>phosphate buffer solution (pH 7.2, 37 °C)<br>5% after 25d / - | no data shown | no data shown |
| oligo(ε-caprolactone)diols, oligo(*p*-dioxanone)diols, and diisocyanate | 7, 77, 78 | third cycle<br>$R_f$ 98 - 99.5%<br>$R_r$ 98 - 99% | aqueous buffer solution (pH 7; 37 °C)<br>270 d [iii]/ - | [iv]<br>no statistical difference on the activity of Matrix Metalloproteinases (MMPs) and Tissue Inhibitor of MMPs (TIMPS) | CAM-test [v]<br>no avascular zones and/or free capillaries |
| multiblock copolymers containing poly(*L*-lactide) and poly[glycolide-*co*-(ε-caprolactone)]-segments | 79 | third cycle<br>$R_f$ ~ 99.0%<br>$R_r$ ~ 99.6% | phosphate buffer solution (pH 7.4; 37 °C)<br>154 d / - | no data shown | no data shown |

[i] 75 wt% poly(ε-caprolactone) ($M_n$ = 3000 g·mol$^{-1}$), 25 wt% poly(ethylene glycol) ($M_n$ = 3000 g·mol$^{-1}$),total $M_n$ = 28.700 g·mol$^{-1}$,gel content 57%
[ii] 75 wt% poly(ε-caprolactone) ($M_n$ = 3000 g·mol$^{-1}$), 25 wt% poly(ethylene glycol) ($M_n$ = 3000 g·mol$^{-1}$),total $M_n$ = 28.700 g·mol$^{-1}$,gel content 57%
[iii] 42 wt% oligo(*p*-dioxanone)
[iv] epithelial cell cultures of the upper aerodigestive tract seeded on a multiblock copolymer material 38 wt% poly(p-dioxanone) and 56 wt% poly(ε-caprolactone)
[v] 38 wt% poly(p-dioxanone) and 56 wt% poly(ε-caprolactone)

When biodegradable polymers are used in medical devices the biocompatibility of the solid polymer and its degradation products has to be considered [69]. Additionally, medical applications require thoroughly sterilization of the materials [70]. Widely accepted low-temperature sterilization techniques for polymerous materials are ethylene oxide (EO) and low-temperature plasma (LTP) sterilization. When the influence of EO and LTP sterilization on an AB-type shape-memory polymer network based on poly(ε-caprolactone) dimethacrylate and n-butyl acrylate was investigated [71], statistically significant differences in the cell lysis in *in vitro* cell-screening tests could be detected [72]. In contrast in chorioallantoic membrane tests (CAM-test) as *in vivo* tests no adverse effects on the angiogenesis, the growing of blood vessels, could be determined [72]. In theses tests a fertilized chicken egg is partly peeled and the polymer sample is placed on the outer skin of the egg in the shell-free area. Afterwards the egg is further incubated. The differences between the *in vitro* and the *in vivo* results have been attributed to remaining EO in the polymer material or silicon particles from the EO sterilization or surface oxidation during LTP sterilization. It can be concluded, that the polymer does not harm the surrounding tissue but proper chose of sterilization technique is important. This positive trend was verified when this material was subcutaneously implanted in male NMRI mice: a remarkable integration in the soft tissue coinciding with an early appearance of blood vessel formation was found [73]. This is notable as these mice named according to their tribe - Naval Medical Research Institute - are lacking of thymus and are therefore especially sensitive for infections. In an animal model the stability and integration into the adjacent tissue was examined [74]. No gas leakage after gas insufflation could be detected and fast and unfavorable degradation of the degradable polymer did not occur. A tight connection between the polymer and the adjacent stomach was found, resulting in an adequate mechanical stability under the extreme pathophysical conditions of the stomach milieu.

In a polyaddition reaction of telechelic oligomers bearing several hydroxylgroups with diisocyanates, covalently crosslinked shape-memory polymers with $T_{trans} = T_g$ were obtained [75]. An isomeric mixture of 1,6-diisocyanato-2,2,4-trimethylhexane and 1,6-diisocyanato-2,4,4-trimethylhexane was used to couple star-shaped oligoesters of *rac*-dilactide and diglycolide. Like in aliphatic copolyesters from diglycolide and dilactide bulk erosion can be observed for this type of polymer. Covalently crosslinked biodegradable polymer networks with $T_{trans} = T_m$ were realized in multiblock copolyesters from poly(ε-caprolactone) and poly(ethlene glycol) and a chain extender based on cinnamic acid groups [76]. Irradiation with light of suitable wavelengths ($\lambda > 280$ nm) resulted in [2 + 2] cycloaddition reaction of the cinnamic acid moieties and forms the covalent crosslinks. Here, the degradation properties can be controlled by the crosslink density, which is controlled by the irradiation time. Additionally was shown that after an induction period, weight loss per day increased with increasing poly(ethylene glycol) content linearly.

Biodegradability was also realized in thermoplastic shape-memory polymers, which have been obtained as linear block copolymers from oligo(ε-caprolactone)diols, oligo(*p*-dioxanone)diols, and diisocyanate as junction unit [7]. Here oligo(ε-caprolactone) acts as crystallizable switching segment, while the phase related to $T_{perm}$ is formed by crystalline oligo(*p*-dioxanone) segments. The presented multiblock copolymers display a linear mass loss *in vitro*, resulting in continuous release of degradation products. In *in vitro* cell seeding tests, no statistical difference could be determined between the shape-memory polymer sample and a polystyrene control sample [77]. This positive result was proven additionally in CAM-tests [78].

Another example of an potentially biodegradable shape-memory polymer are multiblock copolymers containing poly(*L*-lactide) and poly[glycolide-*co*-(ε-caprolactone)]-segments [79]. Here, degradability of the switching segment was increased by incorporation of easily hydrolysable ester bonds with the drawback of non-linear erosion. The biocompatibility has not been shown yet.

Figure 9

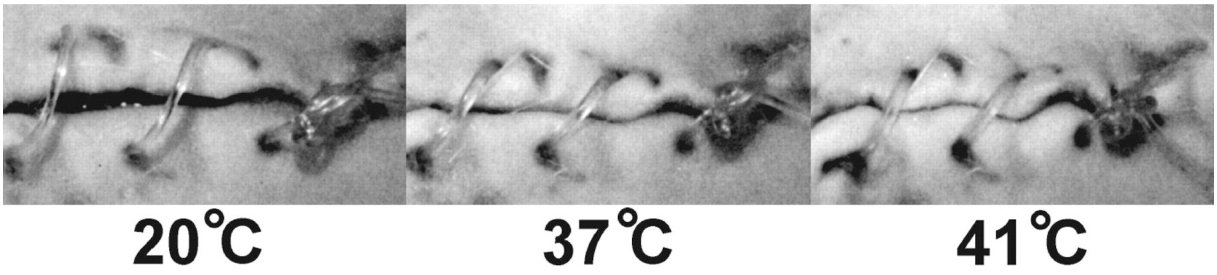


Degradable shape-memory suture for wound closure. The photo series from the animal experiment shows (left to right) the shrinkage of the fiber while temperature increases. (taken from [7])



## *6. Conclusion and outlook*

The field of actively moving polymers, which are able to perform movements by themself, is presently progressing rapidly [9]. Shape-memory polymers play a key role within this field. Fundamental shape-memory research is focussing on the implementation of other stimuli than heat to actuate shape-memory polymers, or to actuate them remotely. First examples have been shown by the light–induced stimulation of shape-memory polymers or the use of alternating magnetic fields for remote actuation. It is assumed that these methods of stimulation will open new fields of application. An important application area for shape-memory polymers are active medical devices and implants [60], where first demonstration objects were already presented [39, 40]. The application requirements can be very complex in this area. Therefore, an actual trend in the development of multifunctional materials can be spotted [66]. Furthermore, there is a strong demand for actively moving material being able to perform complex movements. These requirements could be fulfilled by materials which are able to perform two more predetermined shifts [80].

## *7. References*

1. Hu, J., et al. *Journal of Dong Hua University (Eng. Ed.)*, (2002), **19**, 3.
2. Mondal, S. and Hu, J.L. *Indian Journal of Fibre & Textile Research*, (2006), **31**, 66-71.
3. Charlesby, A., *Atomic Radiation and Polymers*. 1960, Pergamon Press: Oxford. p. 198- 257.

4. Campbell, D., et al. *Elastic Memory Composite Material: An Enabling Technology For Future Furable Space Structures*. in *46th AIAA/ASME/ASCE/AHS/ASC Structures, Structural Dynamics, and Materials Conference*. 2005.
5. Hussein, H. and Harrison, D. *Investigation into the use of engineering polymers as acutators to produce 'automatic disassembly' of electronic products*. in *Design and Manufacture for Sustainable Development 2004*. 2004.
6. Wache, H.M., et al. *Journal of Materials Science-Materials in Medicine*, (2003), **14**, 109-112.
7. Lendlein, A. and Langer, R. *Science*, (2002), **296**, 1673-1676.
8. Metcalfe, A., et al. *Biomaterials*, (2003), **24**, 491-497.
9. Behl, M. and Lendlein, A. *Soft Matter*, (2007), **3**, in press.
10. Hornbogen, E. *Advanced Engineering Materials*, (2006), **8**, 101-106.
11. Lendlein, A. and Kelch, S. *Angewandte Chemie-International Edition*, (2002), **41**, 2034-2057.
12. Lendlein, A., et al., *Shape-Memory Polymers*, in *Encyclopedia of Materials: Science and Technology – Updates*, K.H.J. Buschow, et al., Editors. 2005, Elsevier Science Ltd.: New York.
13. Jiang, H.Y., et al. *Advanced Materials*, (2006), **18**, 1471-1475.
14. Morshedian, J., et al. *Macromolecular Theory and Simulations*, (2005), **14**, 428-434.
15. Liu, Y.P., et al. *International Journal of Plasticity*, (2006), **22**, 279-313.
16. Diani, J., et al. *Polymer Engineering and Science*, (2006), **46**, 486-492.
17. Barot, G. and Rao, I.J. *Zeitschrift Fur Angewandte Mathematik Und Physik*, (2006), **57**, 652-681.
18. Kim, B.K., et al. *Polymer*, (1996), **37**, 5781-5793.
19. Li, F.K., et al. *Journal Of Applied Polymer Science*, (1996), **62**, 631-638.
20. Ma, Z.L., et al. *Journal of Applied Polymer Science*, (1997), **63**, 1511-1515.
21. Jeong, H.M., et al. *Journal Of Materials Science*, (2000), **35**, 279-283.
22. Jeong, H.M., et al. *Polymer*, (2000), **41**, 1849-1855.
23. Ni, X. and Sun, X. *Journal Of Applied Polymer Science*, (2006), **100**, 879-885.
24. Cho, J.W., et al. *Journal Of Applied Polymer Science*, (2004), **93**, 2410-2415.
25. Booth, C.J., et al. *Polymer*, (2006), **47**, 6398-6405.
26. Perez-Foullerat, D., et al. *Macromolecular Chemistry and Physics*, (2004), **205**, 374-382.
27. Kleinhans, G., et al. *Kunststoffe*, (1984), **74**, 445-449.
28. Kleinhans, G. and Heidenhain, F. *Kunststoffe*, (1986), **76**, 1069-1073.
29. Zhu, G., et al. *Journal Of Applied Polymer Science*, (2003), **90**, 1589-1595.
30. Zhu, G.M., et al. *Radiation Physics and Chemistry*, (2006), **75**, 443-448.
31. Li, F.K., et al. *Journal of Applied Polymer Science*, (1999), **71**, 1063-1070.
32. Liu, C.D., et al. *Macromolecules*, (2002), **35**, 9868-9874.
33. Li, F.K. and Larock, R.C. *Journal of Applied Polymer Science*, (2002), **84**, 1533-1543.
34. Kagami, Y., et al. *Macromolecular Rapid Communications*, (1996), **17**, 539-543.
35. Goethals, E.J., et al. *Macromolecular Symposia*, (1998), **132**, 57-64.
36. Reyntjens, W.G., et al. *Macromolecular Rapid Communications*, (1999), **20**, 251-255.
37. Lee, S.H., et al. *Smart Materials & Structures*, (2004), **13**, 1345-1350.
38. Rousseau, I.A. and Mather, P.T. *Journal Of The American Chemical Society*, (2003), **125**, 15300-15301.
39. Maitland, D.J., et al. *Lasers In Surgery And Medicine*, (2002), **30**, 1-11.
40. Small, W., et al. *Optics Express*, (2005), **13**, 8204-8213.
41. Liu, C.D. and Mather, P.T. *ANTEC*, (2003), 1962.
42. Biercuk, M.J., et al. *Applied Physics Letters*, (2002), **80**, 2767-2769.
43. Li, F.K., et al. *Journal of Applied Polymer Science*, (2000), **75**, 68-77.

44. Liang, C., et al. *Journal of Intelligent Material Systems and Structures*, (1997), **8**, 380-386.
45. Gall, K., et al. *Journal of Intelligent Material Systems and Structures*, (2000), **11**, 877-886.
46. Ash, B.J., et al. *Investigation into the thermal mechanical behavior of PMMA/alumina nanocomposites*. 2001.
47. Bhattacharya, S.K. and Tummala, R.R. *Journal of Electronic Packaging*, (2002), **124**, 1-6.
48. Koerner, H., et al. *Nature Materials*, (2004), **3**, 115-120.
49. Cho, J.W., et al. *Macromolecular Rapid Communications*, (2005), **26**, 412-416.
50. Mohr, R., et al. *Proceedings of the National Academy of Sciences of the United States of America*, (2006), **103**, 3540-3545.
51. Buckley, P.R., et al. *Ieee Transactions on Biomedical Engineering*, (2006), **53**, 2075-2083.
52. Yang, B., et al. *Smart Materials & Structures*, (2004), **13**, 191-195.
53. Huang, W.M., et al. *Applied Physics Letters*, (2005), **86**.
54. Yang, B., et al. *Polymer*, (2006), **47**, 1348-1356.
55. Yang, B., et al. *Scripta Materialia*, (2005), **53**, 105-107.
56. Jung, Y.C., et al. *Journal of Macromolecular Science Part B-Physics*, (2006), **45**, 453-461.
57. Lendlein, A., et al. *Nature*, (2005), **434**, 879-882.
58. Yu, Y.L. and Ikeda, T. *Macromolecular Chemistry and Physics*, (2005), **206**, 1705-1708.
59. Langer, R. and Tirrell, D.A. *Nature*, (2004), **428**, 487-492.
60. El Feninat, F., et al. *Advanced Engineering Materials*, (2002), **4**, 91-104.
61. Lendlein, A. and Langer, R.S., Self-expanding device for the gastrointestinal or uro-genital area. 2004. WO 2004073690 A1
62. Marco, D., Biodegradable self-inflating intragastric implants for curbing appetite. 2006. WO 2006/092789 A2
63. Huang, W.M., et al. *Journal of Intelligent Material Systems and Structures*, (2006), **17**, 753-760.
64. Hampikian, J.M., et al. *Materials Science & Engineering C-Biomimetic and Supramolecular Systems*, (2006), **26**, 1373-1379.
65. Fare, S., et al. *Journal of Biomedical Materials Research Part A*, (2005), **73A**, 1-11.
66. Lendlein, A. and Kelch, S. *Functionally Graded Materials Viii*, (2005), **492-493**, 219-223.
67. Tamada, J.A. and Langer, R. *Proceedings of the National Academy of Sciences of the United States of America*, (1993), **90**, 552-556.
68. von Burkersroda, F., et al. *Biomaterials*, (2002), **23**, 4221-4231.
69. Zange, R., et al. *Journal of Controlled Release*, (1998), **56**, 249-258.
70. Wallhäuser, K., *Praxis der sterilization-desinfektion-konservierung*. 5. Auflage ed. (1995): Georg Thieme.
71. Lendlein, A., et al. *Proceedings of the National Academy of Sciences of the United States of America*, (2001), **98**, 842-847.
72. Rickert, D., et al. *Journal of Biomedical Materials Research Part B-Applied Biomaterials*, (2003), **67B**, 722-731.
73. Binzen, E., et al. *Clinical Hemorheology and Microcirculation*, (2004), **30**, 283-288.
74. Rickert, D., et al. *Biomedizinische Technik*, (2006), **51**, 116-124.
75. Alteheld, A., et al. *Angewandte Chemie-International Edition*, (2005), **44**, 1188-1192.
76. Nagata, M. and Kitazima, I. *Colloid and Polymer Science*, (2006), **284**, 380-386.
77. Rickert, D., et al. *Clinical Hemorheology and Microcirculation*, (2005), **32**, 117-128.

78. Rickert, D., et al. *Clinical Hemorheology and Microcirculation*, (2003), **28**, 175-181.
79. Min, C.C., et al. *Polymers for Advanced Technologies*, (2005), **16**, 608-615.
80. Bellin, I., et al. *PNAS*, (2006), **103**, 18043-18047.
81. Lendlein, A., et al. *Kunststoffe International*, (2006), **96**, 54-59.